P4.5 **Performance of LIDAR-based Turbulence Detection Algorithm**

P.W. Chan *
Hong Kong Observatory, Hong Kong, China

K.M. Kwong
Hong Kong Polytechnic University, Hong Kong, China

1. INTRODUCTION

Turbulent airflow occurs in the vicinity of the Hong Kong International Airport (HKIA) when strong background winds from the east to southwest climb over the mountainous Lantau Island to the south of the airport. Low-level turbulence (below 1600 feet or within 3 nautical miles from the runway end, in accordance with the requirement of the International Civil Aviation Organization (ICAO)) could be a hazard to the arriving/departing aircraft. The Hong Kong Observatory (HKO) provides low-level turbulence alerting service for HKIA using the internationally adopted metric of turbulence intensity, viz. cube root of eddy dissipation rate (EDR). Significant turbulence encounters include moderate and severe turbulence, which have the EDR in the region of 0.3 – 0.5 $m^{2/3}s^{-1}$ and greater than 0.5 $m^{2/3}s^{-1}$ respectively.

The Windshear and Turbulence Warning System (WTWS) of HKO estimates the turbulence intensities along the runway corridors of HKIA using the correlation equations established between the aircraft-measured EDR and the wind measurements in Hong Kong mainly in the summer and autumn (between April and November) of a couple of years before the opening of HKIA in 1998. Significant turbulence in the lower troposphere could also occur in east to southeasterly airflow in springtime. Moreover, the installation of LIght Detection And Ranging (LIDAR) systems at HKIA since 2002 offers the possibility of measuring the wind fluctuations and thus turbulence intensity more directly along the glide paths of HKIA. Kwong and Chan (2007) discussed the determination of EDR profile using the glide path scan of the LIDAR (Chan et al., 2006). The EDR profiles so obtained are found to be consistent with the pilot reports of turbulence in selected cases.

This paper focuses on the performance of the LIDAR-based EDR profiles in capturing significant turbulence in some typical episodes of terrain-disrupted turbulent airflow at HKIA. Section 2 gives an overview of the EDR calculation method. The case studies are presented in Section 3. Findings of the study are concluded in Section 4.

2. CALCULATION OF EDR

The technical details of calculating EDR from the azimuthal structure function based on LIDAR's radial velocity data could be found in Kwong and Chan (2007). Only a summary of the major equations will be described here. The 07LA runway corridor (i.e. arriving at the north runway of HKIA from the west, see Figure 1(a)) is considered in the present study. The LIDAR is configured to scan at a rather slow azimuthal rate of 0.8 degree/second over this runway corridor. The glide-path scan of the LIDAR in this corridor is divided into a number of sub-sectors, each has a size of 10 range gates time 16 radials (each radial having an azimuthal span of 0.1 degree or so). For a particular scan k, the radial velocity "surface" within this sub-sector (as a function of range R and azimuth angle θ) is fitted with a plane using singular value decomposition method. The velocity fluctuation $\hat{v}'$ at each point in the space (R, θ) is taken to be the difference between the measured radial velocity $\hat{v}$ and the fitted velocity $\overline{v}$ on the plane:

$$\hat{v}'(R,\theta,k) = \hat{v}(R,\theta,k) - \overline{v}(R,\theta,k)\,. \qquad (1)$$

The azimuthal structure function is calculated:

$$\hat{D}_{AZ}(R\bullet\theta_1, R\bullet\theta_2) = N^{-1}\sum_{R,k}[\hat{v}'(R,\theta_1,k) - \hat{v}'(R,\theta_2,k)]^2 - E(R)\,, \qquad (2)$$

where the summation is made over all the possible azimuthal angles and scans over 15 minutes, and N refers to total number of entries in the summation. The error term E is calculated using the covariance method on the radial velocity difference (Frehlich 2001; Frehlich et al. 2006). The covariance of the velocity estimate is given by:

$$\hat{C}(R,n\Delta\theta) = N^{-1}\sum_{l,k}\hat{v}'(R,l\Delta\theta,k)\times\hat{v}'(R,(l+n)\Delta\theta,k)\,. \qquad (3)$$

And the error term of velocity difference is taken as two times of the error of the velocity estimate:

$$E = 2(\hat{C}(0) - 2\hat{C}(\Delta\theta) + \hat{C}(2\Delta\theta))\,. \qquad (4)$$

$EDR^{1/3}$ is determined by fitting the azimuthal structure function with the theoretical von Kármán model. Let $s = R(\theta_1-\theta_2)$ for two azimuthal angles θ_1 and θ_2. According to Frehlich et al. (2006), for homogeneous von Kármán turbulence over a two-dimensional plane (R, s),

$$D_{AZ}(R,s) = 2\sigma^2[\Lambda(q/L_0) + \Lambda_D(q/L_0)(1-R^2/q^2)], \qquad (5)$$

where $q = (R^2+s^2)^{1/2}$,

$$\Lambda_D(x) = (0.29627426)x^{4/3}K_{2/3}(x)\,, \qquad (6)$$

σ^2 is the variance of the radial velocity, L_0 is the outer scale of turbulence, $\Lambda(x)$ is a universal function, and

* *Corresponding author address:* P.W. Chan, Hong Kong Observatory, 134A Nathan Road, Hong Kong email: pwchan@hko.gov.hk

$K_{2/3}(x)$ is the modified Bessel function of order 2/3. Since the LIDAR is configured to scan in the azimuthal direction very slowly, the transverse dimension of the LIDAR sensing volume for each radial velocity estimate should be much less than the range resolution of about 100 m. As such, Eq. (5) could be simplified to be:

$$D_{AZ}(s,\sigma,L_0) = 2\sigma^2 G_\theta(s/\Delta p,\mu,\chi)\,, \qquad (7)$$

where G_θ is given as Eq. (46) in Frehlich et al. (2006).

The azimuthal structure function is calculated from the LIDAR's radial velocity according to Eq. (2) and then fitted with the theoretical result in Eq. (7) to give σ^2 and L_0. EDR (ε) is given by:

$$\varepsilon = (0.933668)\frac{\sigma^3}{L_0}\,. \qquad (8)$$

The fitting involves the minimization of a cost function to obtain two unknown parameters, namely, the variance of radial velocity and the outer scale of turbulence. To speed up the minimization process, the fitted parameters of the nearest sub-sector are used as the starting point of the minimization for a particular sub-sector or, if the nearest sub-sector values are not available, the fitted parameters of the same sub-sector at the previous moment are used.

3. CASE STUDIES

Three episodes of turbulent airflow at HKIA are studied in this paper. As discussed in Section 1, the EDR algorithm in WTWS was established in tropical cyclone situations. The first case considers the gale-force southeasterly winds brought about by Typhoon Prapiroon in early August 2006 to see how the WTWS $EDR^{1/3}$ compares with the LIDAR-determined $EDR^{1/3}$.

Figure 1(a) shows the radial velocity distribution in the vicinity of HKIA as measured by the LIDAR, when southeasterly winds in excess of 20 m/s prevailed at the airport area. The two sets of $EDR^{1/3}$ data over runway 07LA are compared in the scatter plot in Figure 1(b) and the time series plot of Figure 1(c). The period under consideration is between 1 and 7 August 2006, covering the whole episode when Hong Kong was under the influence of Typhoon Prapiroon. Due to the immense computing power requirement for EDR calculation, the LIDAR-based EDR profile is only updated every 15 minutes, though the glide-path scan data are updated every 2 minutes. Following the approach in Cornman et al. (2006) for turbulence reporting and alerting, the median and the 95 percentage of $EDR^{1/3}$ value of the EDR profile every 15 minutes are used in the time series plot of Figure 1(c). The median value is considered in the scatter plot of Figure 1(b). It could be seen from these two Figures that WTWS $EDR^{1/3}$ and the median of LIDAR-based $EDR^{1/3}$ are very well correlated.

Pilot reports of significant turbulence in this episode are also plotted in Figure 1(c). In order to differentiate the different levels of turbulence as reported by the pilots, the following arbitrary scale is used to plot the turbulence intensity:

- Light turbulence – 1
- Light to moderate turbulence – 1.5
- Moderate turbulence – 2
- Moderate to severe turbulence – 2.5
- Severe turbulence – 3

  (numbers below 1 or above 3 are not used)

The $EDR^{1/3}$ values of WTWS and the LIDAR reach 0.3 $m^{2/3}s^{-1}$ or so later in the day of 2 August 2006. Pilot turbulence reports were not received, but reports of significant windshear (sustained changes of headwind/tailwind of 15 knots or more over a distance of 400 m to 4000 m) started to appear for western approaches to HKIA at about 15 UTC on that day. For terrain-disrupted airflow with rapid wind fluctuations, the pilots may have difficulty in differentiating between windshear and turbulence. Pilot reports of severe turbulence over 07LA were received beginning at 20:47 UTC of 2 August 2006. The $EDR^{1/3}$ value of WTWS reaches 0.5 $m^{2/3}s^{-1}$ at that time. For the LIDAR, the median $EDR^{1/3}$ value is around 0.4 $m^{2/3}s^{-1}$ and the 95-percentile value is occasionally above 0.5 $m^{2/3}s^{-1}$. Pilot reports of significant turbulence were received up to about 05 UTC, 3 August 2006. For the remaining hours of 3 August, the $EDR^{1/3}$ from both WTWS and the LIDAR remain at high values (0.4 $m^{2/3}s^{-1}$ or above), but there were no more pilot reports of turbulence due to significant decrease of flight movements in turbulent airflow.

It could be seen from Figure 1(c) that, for the limited number of pilot reports in the present case, the turbulence intensity level as subjectively perceived by the pilots does not appear to have good correlation with the $EDR^{1/3}$ value from both WTWS and the LIDAR. The LIDAR-based EDR profiles around the moments of pilot reports are given in Figure 1(d). For this typhoon case, the turbulence intensity tends to be higher at the point closer to touchdown (at about 0.25 nautical mile from the runway threshold). Another peak of turbulence intensity is sometimes observed at 1.5 – 2.5 nautical miles away from the threshold, but it does not seem to be persistent.

The second case is a terrain-disrupted airflow event in springtime, namely, on 23 – 24 February 2007. A typical distribution of radial velocity data from the LIDAR is given in Figure 2(a). A fresh to strong southeasterly airstream prevailed in the airport area. However, a wake of weaker/reversed flow was also observed downstream of the tall mountains (up to 1000 m AMSL) of Lantau Island, such as over the sea to the west of HKIA. The WTWS and LIDAR EDR over 07LA runway corridor are compared in Figure 2(b) and (c) for the period 21 to 26 February 2007. It could be seen that the correlation between the two datasets is not so well in comparison to the typhoon case. The correlation coefficient squared is about 0.37 only, which is about half of the value in the episode of Typhoon Prapiroon. From Figure 2(c), the major discrepancy between the two datasets occurs between 00 and 21 UTC of 23 February 2007, when WTWS $EDR^{1/3}$ remained at about 0.25 $m^{2/3}s^{-1}$, whereas LIDAR $EDR^{1/3}$ was mostly at about 0.15 $m^{2/3}s^{-1}$ only. Further study would be carried out using the EDR values as determined from flight data

recorded onboard the transport category commercial aircraft to find out which EDR estimate (WTWS vs. LIDAR) is more accurate.

There were three pilot reports of significant turbulence at 300 feet over 07LA runway in this episode. Interestingly, they were received at the time when the LIDAR $EDR^{1/3}$ showed a sharp rise at about 21 UTC of 23 February. The reports could be captured by LIDAR $EDR^{1/3}$ if a median value of at least 0.25 $m^{2/3}s^{-1}$ *and* a 95-percentile value of at least 0.3 $m^{2/3}s^{-1}$ are adopted for alerting. On the other hand, they were not captured by the WTWS because the WTWS $EDR^{1/3}$ remained below 0.3 $m^{2/3}s^{-1}$ (Figure 2(c)). Among them, there was one report of severe turbulence at about 21:12 UTC, 23 February. The LIDAR EDR profiles around the times of pilot reports are shown in Figure 2(d). In general, turbulence intensity is the highest between 0.5 and 1 nautical mile from the runway threshold, which is generally consistent with the reporting altitude of significant turbulence by the pilots. It reaches a maximum of about 0.43 $m^{2/3}s^{-1}$ at 21:15 UTC, 23 February, close to the time of the severe turbulence report, but the magnitude is smaller than the internationally adopted level of severe turbulence (0.5 $m^{2/3}s^{-1}$).

To examine whether the not-so-well correlation between WTWS and LIDAR EDR only occurs for springtime terrain airflow disruption, another case of terrain-induced wind disturbance in a southeasterly airstream is considered, namely, on 30 June to 1 July 2007. Synoptically, a surface trough of low pressure affected the south China coastal waters, whereas the southeastern part of China was under the influence of a ridge of high pressure extending from the Pacific. The radial velocity distribution from the LIDAR is given in Figure 3(a). Due to disruption by Lantau terrain, small blobs of reverse flow (each with a horizontal size of a few hundred metres) were observed to the southwest of HKIA. The WTWS and LIDAR EDR are compared in Figure 3(b) and (c) in the period 28 June to 3 July 2007. The correlation between the two datasets is even lower in this case, with a correlation coefficient squared of about 0.14 only.

Two pilot reports of moderate turbulence were received at 21:41 and 21:53 UTC, 30 June 2007. As in the previous case, alerting using LIDAR EDR is possible if a median value of at least 0.25 $m^{2/3}s^{-1}$ and a 95-percentile value of at least 0.3 $m^{2/3}s^{-1}$ are adopted. The reports were not captured by WTWS because the WTWS $EDR^{1/3}$ remained below 0.2 $m^{2/3}s^{-1}$ (Figure 3(c)). The LIDAR EDR profiles around the times of pilot reports are shown in Figure 3(d). The $EDR^{1/3}$ values are slightly larger than 0.3 $m^{2/3}s^{-1}$ between about 0.9 and 1.4 nautical miles from the runway threshold.

4. CONCLUSIONS

Performance of LIDAR-based EDR profile (determined from the azimuthal structure function) in alerting low-level turbulence at HKIA is studied in this paper using three examples. Though in general the LIDAR $EDR^{1/3}$ value does not show good correlation with the turbulence intensity as subjectively perceived by the pilots, it is able to capture the pilot reports if a median value of at least 0.25 $m^{2/3}s^{-1}$ and a 95-percentile value of at least 0.3 $m^{2/3}s^{-1}$ are adopted in the alerting. It is noted that in the Typhoon Prapiroon case, for the periods with LIDAR-derived $EDR^{1/3}$ fulfilling these criteria, there may not be significant turbulence reports from the pilots, which may be due to the difficulty in differentiating between windshear and turbulence for rapid wind fluctuations in terrain-disrupted airflow. Further study would be carried out using the EDR determined from flight data recorded onboard the transport category commercial aircraft. In comparison to pilot turbulence reports, the EDR dataset from the flight data would be more objective in determining the turbulence alerting criteria based on the LIDAR-derived EDR.

The two sets of $EDR^{1/3}$ data for 07LA runway corridor, namely, from WTWS and LIDAR, are compared in the three cases under consideration in this paper. It is found that the correlation between the two datasets is much better in the typhoon event than the non-typhoon events.

To put the LIDAR EDR profile into operation, there are still at least a couple of challenges to be overcome. First of all, the alerting thresholds for the median and the 95 percentile values have to be better established using more cases of turbulent as well as non-turbulent airflow at HKIA. Secondly, the calculation of LIDAR EDR is computationally very intensive. Most of the computation time is spent on the minimization of the cost function to determine σ^2 and L_0 in Eq. (8). More efficient ways to do the minimization are yet to be developed.

Acknowledgement

The authors would like to thank Mr. C.M. Li of the Hong Kong Observatory to compute the EDR profiles for the three case studies in this paper.

References

Chan, P.W., C.M. Shun and K.C. Wu, 2006: Operational LIDAR-based system for automatic windshear alerting at the Hong Kong International Airport. *12th Conference on Aviation, Range, and Aerospace Meteorology*, American Meteorological Society, Georgia, U.S.A.

Cornman, L.B., G. Meymaris, and M. Limber, 2006: An update of the FAA Aviation Weather Research Program's *in situ* turbulence measurement and reporting system. *12th Conference on Aviation, Range, and Aerospace Meteorology*, American Meteorological Society, Georgia, U.S.A.

Frehlich, R.G., 2001: Estimation of velocity error for Doppler lidar measurements. *J. Atmos. Oceanic Technol.*, **18**, 1628–1639

Frehlich, R.G. et al., 2006: Measurements of boundary layer profiles in an urban environment. *J. Appl. Meteor. and Climat.*, **45**, 821-837

Kwong, K.M., and P.W. Chan, 2007: LIDAR-based turbulence intensity calculation along glide paths. *14th Coherent Laser Radar Conference*, Snowmass, Colorado, U.S.A.

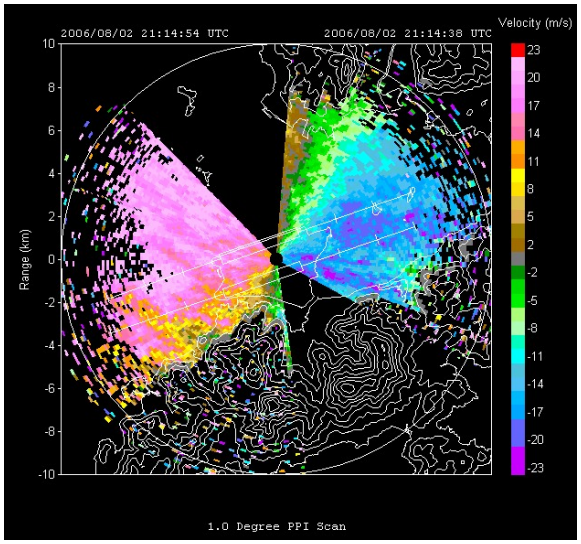

(a)

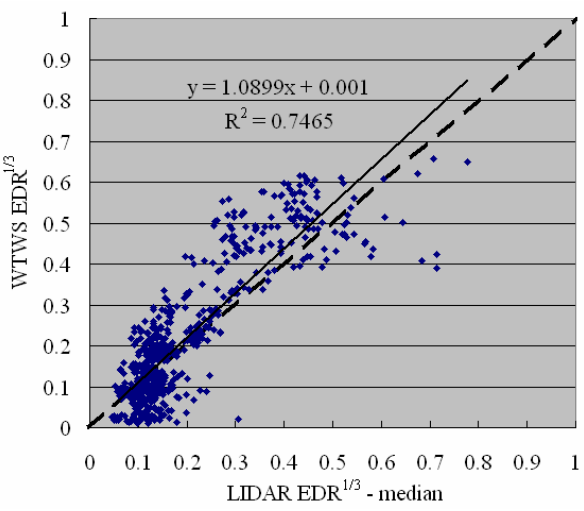

(b)

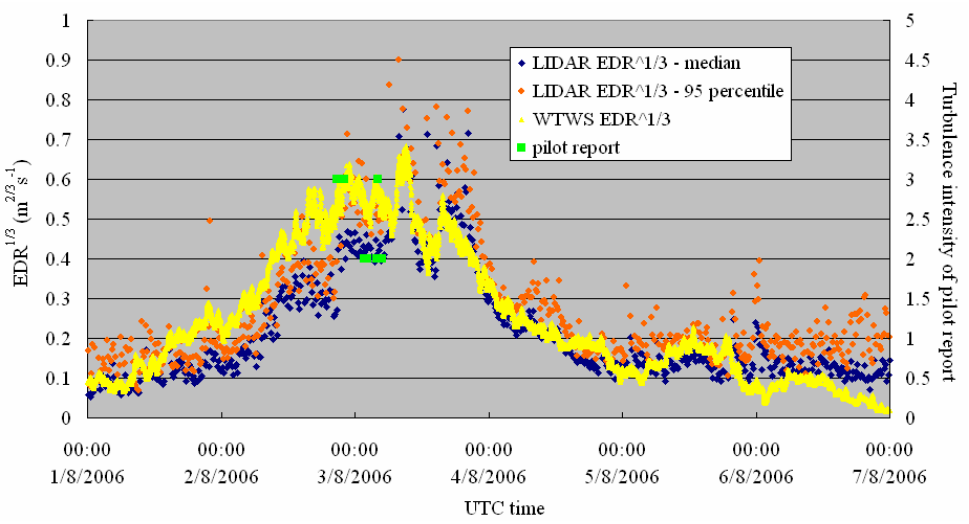

(c)

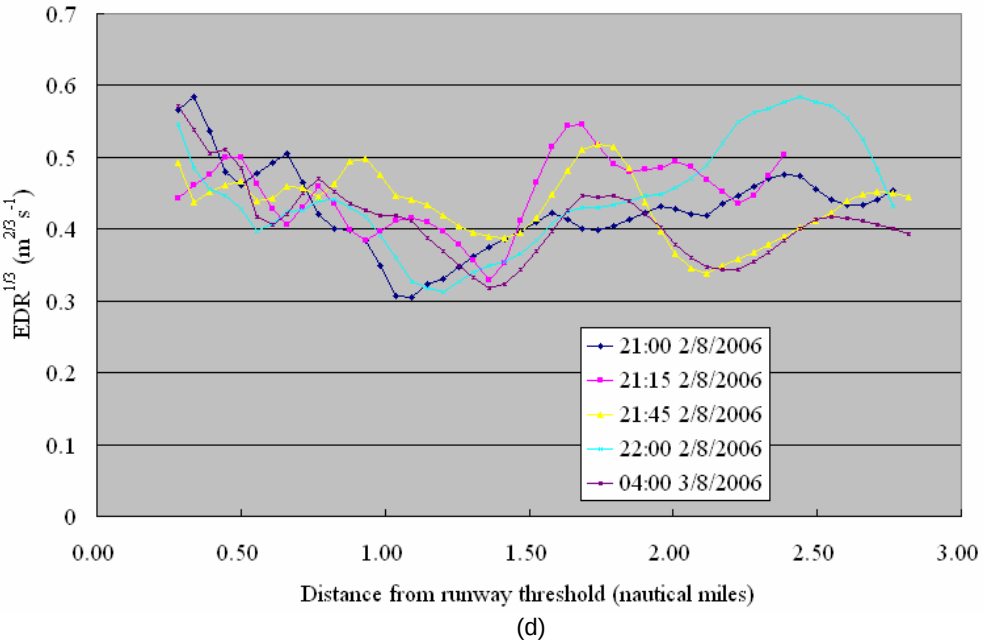

(d)

Figure 1 For the episode of turbulent airflow at HKIA in early August 2007: (a) a typical LIDAR velocity image, (b) scatter plot between WTWS and LIDAR $EDR^{1/3}$, (c) time series of WTWS and LIDAR $EDR^{1/3}$ as well as times of pilot reports, and (d) LIDAR EDR profiles around the times of pilot reports.

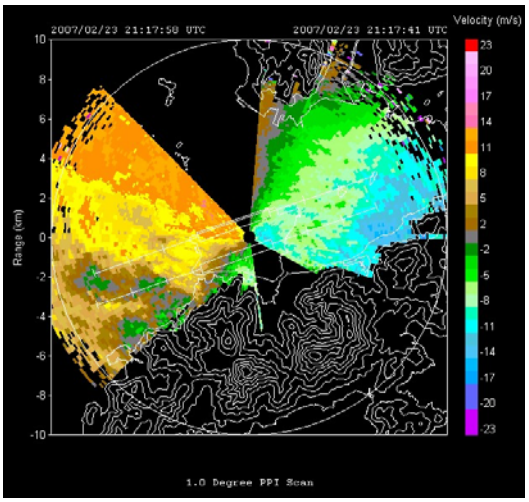

(a)

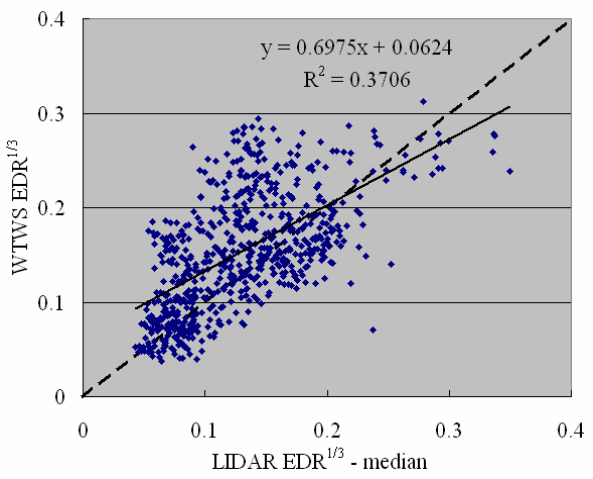

(b)

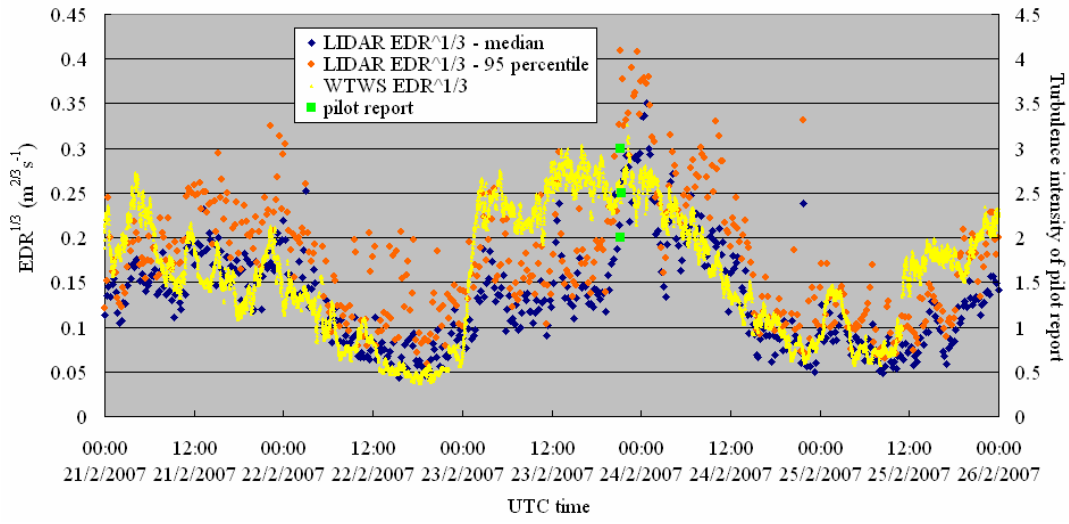

(c)

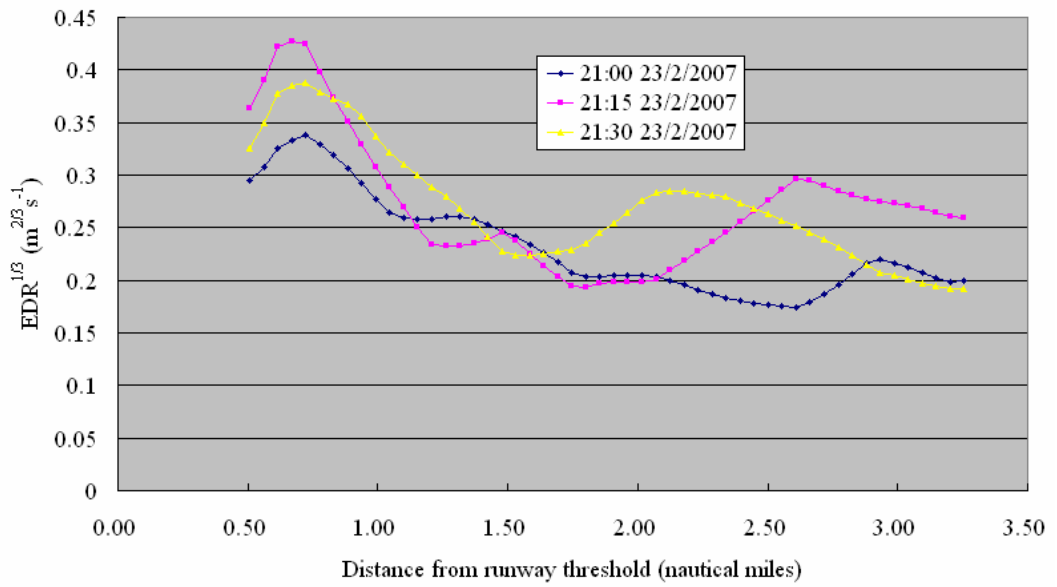

(d)

Figure 2 Same as Figure 1 but for the episode of turbulent airflow at HKIA in late February 2007.

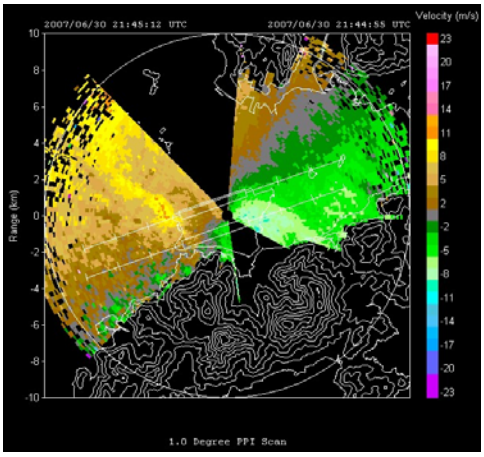

(a)

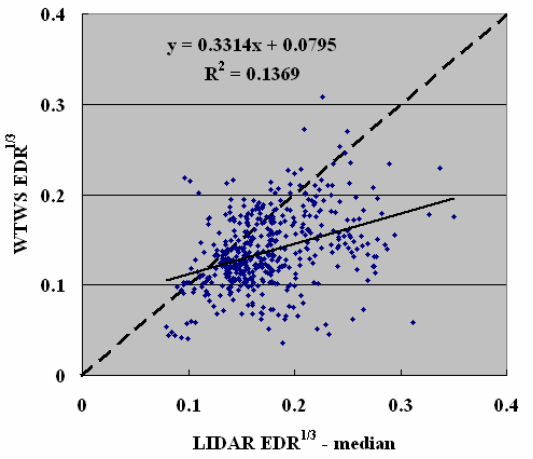

(b)

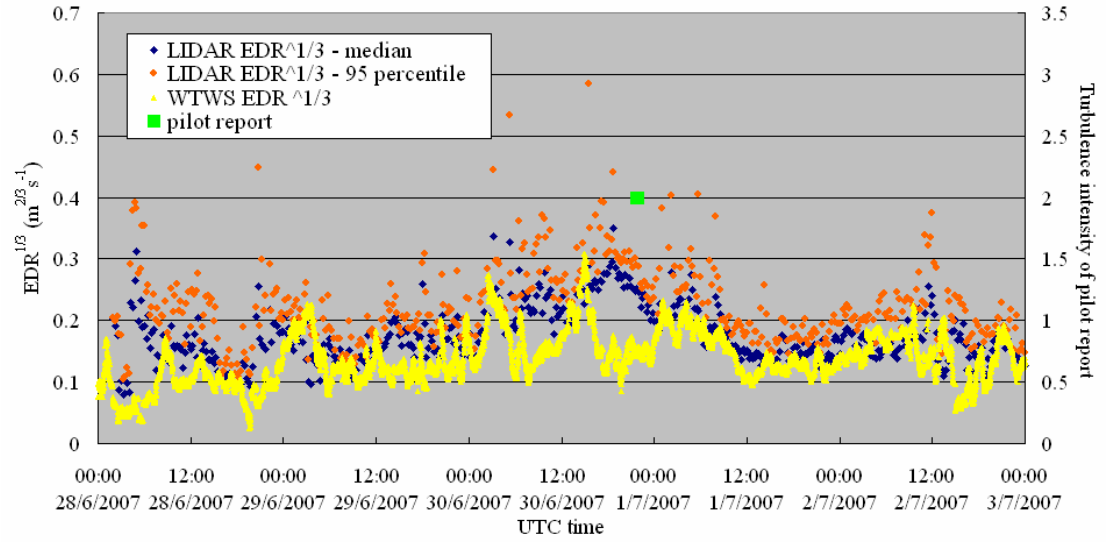

(c)

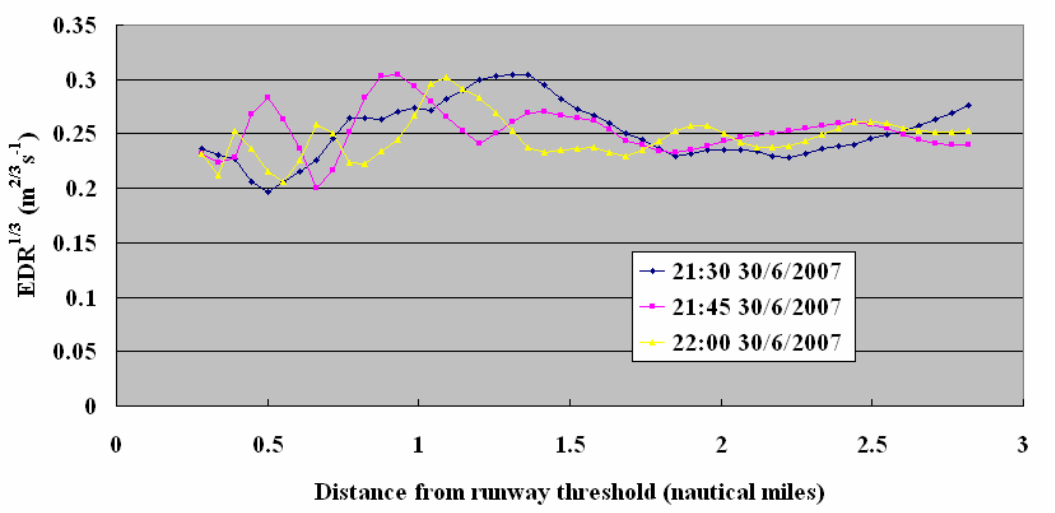

(d)

Figure 3 Same as Figure 1 but for the episode of turbulent airflow at HKIA in late June/early July 2007.